Proceedings of the 2007 American Control Conference
Marriott Marquis Hotel at Times Square
New York City, USA, July 11-13, 2007

ThB03.2

An Application of Active Disturbance Rejection Control
to Self-Sensing Magnetic Bearings[1]

B. X. S. Alexander[2], *Student Member, IEEE*, Richard Rarick[2], *Student Member, IEEE*, Lili Dong[2], *Member, IEEE*

Abstract—**A linearized model of a self-sensing magnetic bearing used in a flywheel energy storage application is analyzed, and an intrinsic feedback mechanism is identified. Based on the model, a cascaded-loop controller is designed using a novel control design technique which actively rejects external disturbances, taking advantage of the feedback mechanism. Simulation results of force-disturbance rejection performance are presented.**

I. INTRODUCTION

Magnetic bearings have been used to achieve non-contact suspension of a flywheel rotor, thus eliminating issues of friction and wear associated with high speed applications using mechanical bearings. The suspension is achieved through an opposing set of electromagnets between which the rotor is positioned. This is shown in Fig. 1 [1].
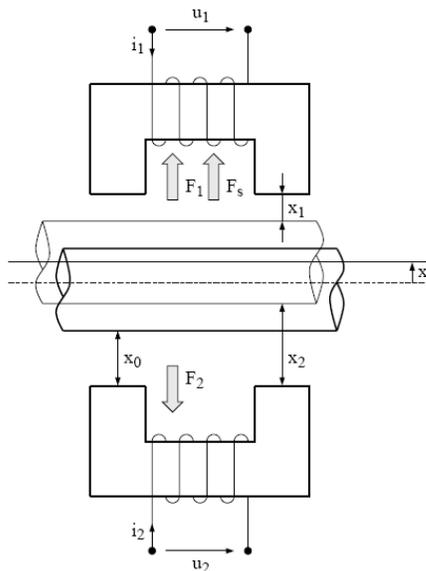

Fig. 1. Magnetic bearing model (one-dimensional)

The position of the rotor can be controlled via the magnetic forces, and the forces can be regulated by adjusting the magnet coil voltage or current.. The magnetic forces exert attractive forces on the rotor shaft, and for this reason magnetic bearings are inherently unstable and require closed-loop control, as will be explained in Section III.

Numerous advanced controller design approaches have been proposed. A linear-quadratic design is used for the pendulous supported flywheel in [2]. An eigenstructure assignment is used for the control of suspension systems for rotating machinery within a magnetic field [3]. A sliding-mode control of a rigid motor via magnetic bearings is introduced in [4]. The modal control of a flexible rotor is given in [5]. In [6], an integral type servo-controlled design using the solution of a linear quadratic regulator problem for a horizontal rotor-magnetic-bearing system is used. And in [7], magnetic bearing control using fuzzy logic is considered. These proposed controllers are often of such complexity that the tuning process is rendered very difficult. The PID controller, however, benefiting from its ease of use, is by far the most prevalent controller used for active magnetic bearing control in industry.

A self-sensing magnetic bearing is a special type of magnetic bearing in that the rotor position information is deduced from the electromagnetic interaction between the stator and rotor [1]. The feedback is based solely on the measured current in the electromagnets, making it possible to design the bearing system without position sensors. This results in a significant advantage because of a considerable reduction in manufacturing costs and the complexity of the system, as well as the elimination of the failure modes associated with the sensors. A self-sensing magnetic bearing with linear control was first proposed in [8]. A linearized model of the self-sensing magnetic bearing was also developed in [1], but the results suggested that the proposed configuration resulted in poor robustness and disturbance rejection. Subsequent experiments have confirmed this view ([9], [10]). In particular, disturbance to the system caused by rotor imbalance is commonly encountered, since imperfections in rotor design and manufacture cannot be avoided. Yet the authors have not found any studies which propose a feasible solution to the disturbance rejection issue of self-sensing bearings.

Based on the linearized model in [1], we have designed a cascaded-loop control structure for controlling rotor position. The primary objective of the present work is to demonstrate the ability of this control to reject an external step force applied to the rotor. Specifically, the control objective is to maintain the deviation of the rotor position close to zero in the presence of the disturbance. We identify an intrinsic feedback in the model in [1], which is then used to deduce the rotor position deviation. We apply a novel control strategy first developed in [11] and [12] that actively rejects disturbances in the system.

The paper is organized as follows. In Section II of the paper, the physical model in [1] is analyzed, and the intrinsic feedback of the system identified. A cascaded-loop control structure is designed in Section III. The control strategy in [11] and [12], called Active Disturbance Rejection Control (ADRC), is introduced in Section IV and integrated into the cascaded-loop structure. Lastly, simulation results are shown in Section V.

II. PLANT MODELING

The nonlinear model of a self-sensing magnetic bearing used for our analysis was developed in [1]. It is based on the configuration in Fig. 1. Two identical, U-shaped electromagnets produce opposing forces, F_1 and F_2, that act on the shaft, thus levitating the rotor, which is ideally positioned midway between the magnets at its unstable equilibrium position, x_0. The deviation of the shaft from the equilibrium position is represented by the displacement x. The distances x_1 and x_2 are the air gap distances between the shaft and the magnets.

The magnetic forces F_1 and F_2 are actuated by the coil currents i_1 and i_2, respectively. The currents, in turn, are controlled via the corresponding voltage drops, u_1 and u_2, across the coils. The main disturbances to the plant considered in this model are external forces such as would occur to a flywheel mounted to a moving vehicle, and rotor imbalance, viewed as an external disturbance. These forces are represented in the aggregate by F_S. The mathematical model of the system is given by the following equations:

$$m\ddot{x} = F_1 - F_2 + F_S \qquad (1)$$

$$F_k = \frac{K}{4}\left(\frac{i_k}{x_k}\right)^2, \qquad k = 1, 2 \qquad (2)$$

$$u_k = Ri_k + L_S \frac{di_k}{dt} + \frac{K}{2}\frac{d}{dt}\left(\frac{i_k}{x_k}\right), \qquad k = 1, 2 \qquad (3)$$

where

$$K = \mu_0 N^2 A \qquad (4)$$

Here m is the mass of the rotor, R is the coil resistance, L_S is the coil self-inductance, μ_0 is the permeability of free space, N is the number of turns in the coil, and A is the area of the magnetic core. The Newtonian equation of motion for the rotor is given in (1). The equations in (2) describe the magnetic forces produced by the bearing as a function of the coil current and air gap distance. And the equation in (3) is determined from Kirchhoff's Voltage Law for the coil circuit. The first term on right hand side of (3) represents the voltage drop caused by coil resistance. The second term models the voltage drop caused by the coil self-inductance, L_S. And the

third term represents the back-Electromotive Force (back-EMF) created by variations in air gap flux and is determined using Ampere's Law and Faraday's Law

When the rotor has been levitated to its equilibrium position, x_0, the bias or nominal current in the electromagnets will be i_0, and the corresponding voltage will be

$$u_0 = Ri_0 \qquad (5)$$

The deviations, i, u, and x, from the nominal equilibrium values give rise to the following relations:

$$\begin{aligned} i_1 &= i_0 + i & i_2 &= i_0 - i \\ u_1 &= u_0 + u & u_2 &= u_0 - u \\ x_1 &= x_0 - x & x_2 &= x_0 + x. \end{aligned} \qquad (6)$$

Noteworthy are the symmetries in the relations, particularly for the coil control voltages. A voltage increase in one coil must be accompanied by a voltage decrease of the same magnitude in the other coil. This symmetry reduces the task of controlling the two inputs, u_1 and u_2, to that of controlling only one input u.

Equations (2) and (3) can be linearized about the operating point (x_0, i_0, u_0) according to the conditions in (6). The result of linearization is a multiple-input, multiple-output (MIMO) plant. The MIMO plant can be divided into two single-input, single-output (SISO) plants [1]. The first plant is obtained by defining a system state vector $\mathbf{x}$ as

$$\mathbf{x} = \begin{bmatrix} x & v & i \end{bmatrix}^T, \qquad (7)$$

where x is the shaft displacement, v is the shaft velocity, and i is the coil current; and by defining the constants k_S, k_I, and L_0 as

$$k_S = \frac{K}{2}\frac{i_0^2}{x_0^3}, \quad k_I = \frac{K}{2}\frac{i_0}{x_0^2}, \quad L_0 = \frac{K}{2x_0}. \qquad (8)$$

With these definitions, the linearized plant is given by the third-order state equation

$$\dot{\mathbf{x}} = \begin{bmatrix} 0 & 1 & 0 \\ \dfrac{2k_S}{m} & 0 & \dfrac{2k_I}{m} \\ 0 & \dfrac{-k_I}{L_S + L_0} & \dfrac{-R}{L_S + L_0} \end{bmatrix}\mathbf{x} + \begin{bmatrix} 0 \\ 0 \\ \dfrac{1}{L_S + L_0} \end{bmatrix}u + \begin{bmatrix} 0 \\ \dfrac{1}{m} \\ 0 \end{bmatrix}F_S. \qquad (9)$$

Note that in Equation (9), the disturbance input, F_S, is not a control input, and therefore the system is a SISO plant.

The second plant is a first-order SISO plant given by the equation for the equilibrium current,

$$\frac{di_0}{dt} = \frac{-R}{L_S + L_0} i_0 + \frac{1}{L_S + L_0} u_0 . \tag{10}$$

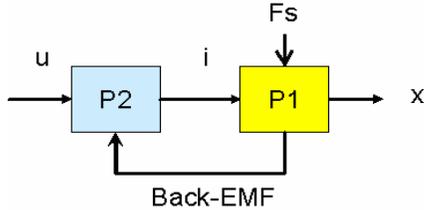Equation (9) can be represented by the following block diagram:

Fig. 2. Block diagram of the linearized system

In Fig. 2, the dynamics of plant P1 is given by the equation

$$\ddot{x} = \frac{2k_S}{m} x + \frac{2k_I}{m} i + \frac{1}{m} F_S . \tag{11}$$

The dynamics of plant P2 is given by

$$\frac{di}{dt} = \frac{-k_I}{L_S + L_0} v + \frac{-R}{L_S + L_0} i + \frac{1}{L_S + L_0} u . \tag{12}$$

In (12) the product of the constant k_I and the velocity, $k_I v$, is the back-EMF voltage which results from changes in the air gap flux. A force disturbance, F_S, on the rotor will affect its velocity and hence the back-EMF voltage. Thus the back-EMF constitutes an intrinsic feedback mechanism, which can be used to deduce the deviation of the rotor position from the operating point.

III. CONTROL STRATEGY

The magnetic bearing plant is open-loop unstable because the magnetic bearings exert *attractive* forces on the rotor shaft that depend on the inverse of the square of the air gap distances. From Fig. 1, it can be seen that any movement of the rotor shaft in a direction away from the equilibrium position, and toward one of the magnets, increases the magnetic force in that direction, and decreases the magnetic force in the opposite direction. Thus the rotor is accelerated away from the equilibrium position. The air gap is normally on the order of a millimeter, thus a disturbance force can cause the rotor to contact the bearing surface and trigger a catastrophic failure. The control objective, then, is to maintain the deviation, *x*, of the rotor from its equilibrium position as close to $x = 0$ as possible in the presence of an external disturbance without the use of a position sensor.

We will only consider the case in which the rotor is initially levitated and in equilibrium, and hence a measurement of the initial conditions for the state-space gives $x = v = i = 0$. Since there is no position sensor, only the coil current is available as a feedback signal. The actuator signal is the coil control voltage *u*. The full dynamics of the bearing plant, linearized about the equilibrium operating point, is characterized by (9) and (10). The value of the equilibrium current is determined by (10). In many magnetic bearing applications, the value of the equilibrium current is fixed to optimize the power consumption.

The proposed controller has a cascaded-loop structure as shown in Fig. 3. The controller C1 is a PD control which uses a displacement set-point and the output of a standard Luenberger state observer (not shown) designed to control the current set-point i^*. This type of control structure is well-known, so it will not be addressed further in this study. Since the rotor displacement is not directly available as a measurement, the Luenberger observer is employed to extract displacement information from the coil current *i* and the control voltage *u*, and this information is used for an estimate of the current set-point i^*. The plant P1 is subjected to an external force disturbance, F_S, as indicated in Fig. 3.

The controller C2 is specifically designed to control the plant P2 using current feedback. Note that P2 also receives back-EMF from P1. The control objective of C2 is to regulate the coil current to the specified set point value i^*. The output signal of C2 is the control voltage across the coils . The design of the controller C2 will be the focus of the subsequent sections, where ADRC will be applied.
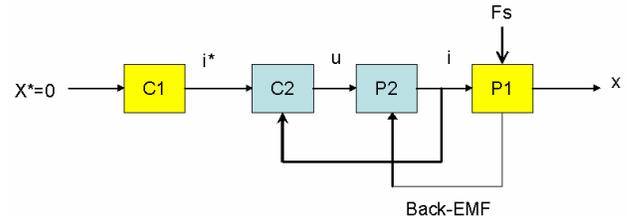

Fig. 3. Illustration of cascaded loop concept

IV. DESIGN USING ACTIVE DISTURBANCE REJECTION CONTROL (ADRC)

The dynamics of the plant P2 is given by (12), which is a first-order system. An external force disturbance will affect the back-EMF term. The fundamental idea of ADRC is to design an observer that estimates any deviation of the plant P2 from a nominal first order plant and compensates for it in real time. Such an observer has been termed an *Extended State Observer* (ESO) [11]. After compensation via the ESO, the nominal first-order plant can be controlled using a proportional controller.

To design the ESO, (12) is rendered into the following standard form:

$$\dot{y} = f(y,v,t) + bu \qquad (13)$$

where $y = i$,

$$f = \frac{-k_I}{L_S + L_0}v + \frac{-R}{L_S + L_0}y, \qquad (14)$$

and

$$b = \frac{1}{L_S + L_0}. \qquad (15)$$

The term f in (13) is referred to as a *generalized disturbance* [12]. It represents the deviation of the plant in Equation (13) from a nominal first-order plant. The ESO contains two state space variables:

$$z_1 = i, \quad z_2 = f. \qquad (16)$$

Here the first-order state space has been augmented or extended with an additional state, namely, $z_2 = f$. If we let $y = z_1$, then Equation (13) can written as:

$$\dot{z}_1 = z_2 + \frac{1}{L_S + L_0}u. \qquad (17)$$

And if we let h be the time derivative of f, then $\dot{z}_2 = h$, and the corresponding matrix state space model is

$$\begin{aligned} \dot{\mathbf{z}} &= \mathbf{A}\mathbf{z} + \mathbf{B}u + \mathbf{E}h \\ y &= \mathbf{C}\mathbf{z} \end{aligned} \qquad (18)$$

where

$$\mathbf{A} = \begin{bmatrix} 0 & 1 \\ 0 & 0 \end{bmatrix}, \ \mathbf{B} = \begin{bmatrix} \frac{1}{L_s + L_0} \\ 0 \end{bmatrix}, \ \mathbf{C} = \begin{bmatrix} 1 \\ 0 \end{bmatrix}^T, \ \mathbf{E} = \begin{bmatrix} 0 \\ 1 \end{bmatrix} \qquad (19)$$

The generalized disturbance, $z_2 = f$, can now be estimated by the ESO, which has the following construction:

$$\begin{aligned} \dot{\hat{\mathbf{z}}} &= \mathbf{A}\hat{\mathbf{z}} + \mathbf{B}u + \mathbf{L}(y - \hat{y}) \\ &= \mathbf{A}\hat{\mathbf{z}} + \mathbf{B}u + \mathbf{L}y - \mathbf{L}\hat{y}. \end{aligned} \qquad (20)$$

The state of this observer, $[\hat{z}_1, \hat{z}_2]^T$, corresponds to the estimated values of the quantities:

$$\hat{z}_1 \approx z_1, \quad \hat{z}_2 \approx f. \qquad (21)$$

Equation (20) can be simplified using the relation $\hat{y} = \mathbf{C}\hat{\mathbf{z}}$, and is rewritten as

$$\begin{aligned} \dot{\hat{\mathbf{z}}} &= \mathbf{A}\hat{\mathbf{z}} + \mathbf{B}u + \mathbf{L}y - \mathbf{L}\mathbf{C}\hat{\mathbf{z}} \\ &= (\mathbf{A} - \mathbf{L}\mathbf{C})\hat{\mathbf{z}} + \mathbf{B}u + \mathbf{L}y, \end{aligned} \qquad (22)$$

where the observer gain vector $\mathbf{L}$ and the characteristic equation of the observer matrix are given by

$$\mathbf{L} = [\beta_1, \beta_2]^T \qquad (23)$$

and

$$\det|\mathbf{A} - \mathbf{L}\mathbf{C} - s\mathbf{I}| = s^2 + \beta_1 s + \beta_2 = 0. \qquad (24)$$

It can be shown that the system in Equations (18) and (19) is observable, so the observer gain $\mathbf{L}$ can be chosen so that (24) has multiple real roots at $-\omega_o$. Under this constraint, we have

$$s^2 + \beta_1 s + \beta_2 = (s + \omega_o)^2 = s^2 + 2\omega_o s + \omega_o^2, \qquad (25)$$

and so

$$\beta_1 = 2\omega_o, \quad \beta_2 = \omega_o^2. \qquad (26)$$

Because the eigenvalues in (24) are all located in the left-half plane, the stability of the observer in (22) is guaranteed. The quantity, ω_o, is referred to as the *observer bandwidth* [12]. This parameterization reduces the number of observer tuning parameters to one. With the ESO properly designed, the ADRC control law is given by

$$u = \frac{1}{b}[-\hat{z}_2 + k_p(i^* - \hat{z}_1)]. \qquad (27)$$

In (27), the first term $\hat{z}_2$ compensates for the generalized disturbance f. This term effectively reduces (13) to a single integrator. The second term of (27) represents the proportional controller with gain k_p.

Tuning of the ADRC controller involves two parameters: the observer bandwidth, ω_o, which adjusts the performance of the disturbance compensation, and the proportional controller gain k_p, which affects set-point tracking. The observer and controller can be tuned separately by adjusting their respective bandwidths. It is recommended that the observer bandwidth be three times higher than the controller gain, if possible [12]. By keeping this relationship between the observer bandwidth and the controller gain, the number of tuning parameters is effectively reduced to one. This constitutes a major simplification in the tuning effort of controller C2.

V. SIMULATION

The effectiveness of the cascaded control structure (Fig. 3) under a constant force disturbance was assessed in simulation. The linearized plant was constructed according to (9). The controller C2 was constructed according to the ADRC control law in (27), while for the controller C1, a simple PD controller was used on the output of the Luenberger observer. The plant parameters were selected according to the physical model described in [1]. The bias current is $i_0 = 1\text{A}$.

The controller gains of the PD are $k_P = 100$, and $k_D = 1000$. The ADRC controller has the gains $\omega_o = 300$ and $\omega_c = 100$, in keeping with the rule of thumb suggested by [12], where ω_c is the gain k_p in (27). The simulation was run for 20 seconds. A constant disturbance force of a magnitude of $F_S = -10$ N was applied to the plant at $t = 2$ seconds. A saturation block for the actuator voltage was included and to keep the voltage between $+5$ and -5 volts.
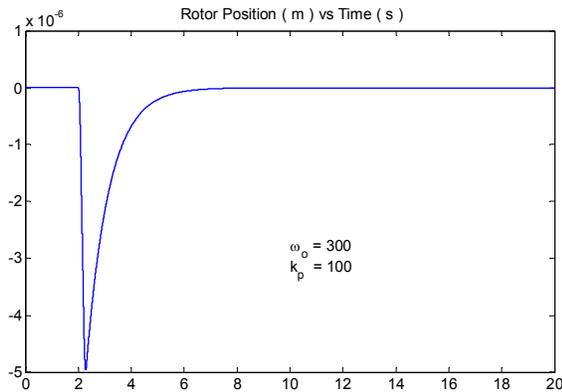

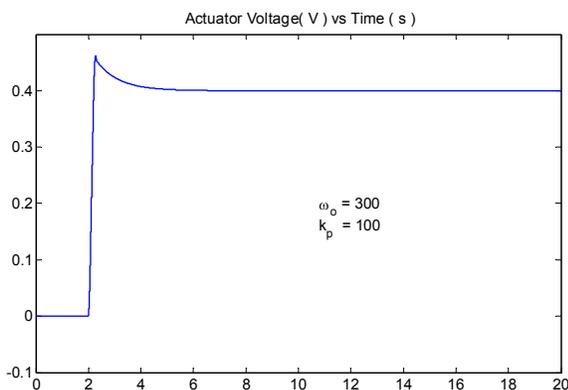Fig. 4. Rotor Position Deviation

Fig. 5. Actuator Voltage Deviation

Fig. 4 and Fig. 5 show that the disturbance force causes the rotor to deviate from its equilibrium position by about -5×10^{-6} meter and return to the equilibrium position in about 4 seconds. The actuator voltage exhibits some overshoot, settling to about 0.4 volts in amplitude in about 4 seconds.

VI. CONCLUSIONS

Self-sensing magnetic bearings have the benefit of low manufacturing costs, but suffer seriously from poor disturbance force rejection capabilities. By analyzing the linearized model of the self-sensing bearing provided in [1], we have identified the back-EMF as a direct effect caused by the external disturbance force. Our cascaded control loop structure effectively rejects the external disturbance force completely through the incorporation of ADRC, which compensates for the disturbance based on the back-EMF.

Our initial simulation results demonstrate that the proposed cascaded loop structure is a viable solution to the long-standing disturbance rejection issue of self-sensing magnetic bearings. Future work on the control of a self-sensing magnetic bearing will be aimed at reducing the settling time in the recovery from the disturbance force and minimizing the overshoot in the actuator voltage. Additional test with a sinusoidal disturbance are also needed.

REFERENCES

[1]   Kucera, "Robustness of Self-Sensing Magnetic Bearing," *Proceedings of the Magnetic Bearings Industrial Conference*, pp. 261-270, 1997
[2]   Hubbard et al., "Feedback control systems for flywheel radial instabilities," *1980 Flywheel Technology Symposium Proceedings*, 1980, pp. 209-17
[3]   Stanway et al., "State variable feedback control of rotor bearing suspension systems." *Proceedings of the Third International Conference on Vibrations in Rotating Machinery*, University of York, 1984, C277/84.
[4]   Sinha et al., "Sliding mode control of a rigid rotor via magnetic bearing," *ASME Biennial Conference on Mechanical Vibration and Noise*, Miami, Florida, September 1991.
[5]   Salm et al., "Modeling and control of a flexible rotor with magnet bearings," *Proceedings of the Third International Conference on Vibrations in Rotating Machinery*, 1984.
[6]   Matsumura et al., "System modeling and control design of a horizontal-shaft magnetic bearing system," *IEEE Transactions on Magnetics*, Vol. 22, pp. 196-203, 1995.
[7]   Hung, "Magnetic bearing control using fuzzy logic." *IEEE Transactions on Industry Applications*, vol. 31, pp. 1492-97, 1996
[8]   Vischer and Bleuler, "Self-sensing active magnetic levitation," *IEEE Transactions on Magnetics*, Vol. 29, 1993.
[9]   Malsen, Montie, Iwaski, "Robustness limitations in self-sensing magnetic bearings," to appear in *ASME Journal of Dynamics, Measurement and Control*, 2005.
[10] Thibeault, Smith, "Magnetic bearing measurement configurations and associated robustness and performance limitations." *ASME Journal of Dynamics, Measurement and Control*, vol. 124, pp. 589-598, Dec. 2002.
[11] Han, "A class of extended state observers for uncertain systems," *Control and Decision*, pp. 85-88, 1995.
[12] Gao, "Scaling and bandwidth-parameterization based controller tuning," *Proceeding of IEEE American Control Conference*, 2003.